

See discussions, stats, and author profiles for this publication at: <https://www.researchgate.net/publication/26660473>

Coordination of (Glycyl)(n)glycine ($n=1-3$) to Co(+) and Co(2+)

ARTICLE *in* THE JOURNAL OF PHYSICAL CHEMISTRY A · AUGUST 2009

Impact Factor: 2.69 · DOI: 10.1021/jp901179t · Source: PubMed

CITATIONS

7

READS

66

4 AUTHORS, INCLUDING:



Albert Rimola

Autonomous University of Barcelona

61 PUBLICATIONS 1,185 CITATIONS

[SEE PROFILE](#)



Mariona Sodupe

Autonomous University of Barcelona

189 PUBLICATIONS 4,600 CITATIONS

[SEE PROFILE](#)



Luis Rodríguez-Santiago

Autonomous University of Barcelona

73 PUBLICATIONS 1,671 CITATIONS

[SEE PROFILE](#)

Coordination of (Glycyl)_nglycine ($n = 1–3$) to Co⁺ and Co²⁺

Erika Constantino, Albert Rimola, Mariona Sodupe,* and Luis Rodríguez-Santiago*

Departament de Química, Universitat Autònoma de Barcelona, Bellaterra 08193, Spain

Received: February 9, 2009; Revised Manuscript Received: June 11, 2009

This paper analyses the interaction of Co⁺ (d⁸, ¹G, and ³F) and Co²⁺ (d⁷, ⁴F) cations with (glycyl)_nglycine ($n = 1–3$) oligomers. The structure, relative energies, and binding energies of the complexes formed have been theoretically determined by means of density functional methods. For all Co⁺ complexes the ground spin state is the triplet one and the most stable structures show tricoordinated geometries. In contrast, for Co²⁺ systems the lowest energy structures are tricoordinated ($n = 1$), tetracoordinated ($n = 2$), and pentacoordinated ($n = 3$). For both cobalt cations, interaction energies increase with the peptide length. Differences in the coordination properties of the ligands are discussed according to their length as well as to the electronic configuration of the metal cation, and results are compared to those previously obtained for the analogous Cu^{+2+/2-} systems. The IR spectra of the most stable and low energy conformers have been simulated, and a discussion of the main vibrational features is provided.

Introduction

Many important biological processes ultimately involve an interaction between metal cations and protein amino acid residues. The study of these systems in the gas phase allows information on their intrinsic physicochemical properties to be obtained, which may help to understand their biological relevance. As a result, and thanks to recent advances in mass spectrometry, the gas phase study of complexes derived from the interaction of metal cations with amino acids and peptides has experienced significant growth during the last two decades. Particularly interesting is the coupling of mass spectrometry with infrared techniques in order to obtain the infrared spectra of charged species in the gas phase. In this sense, IRMPD (infrared multiphoton dissociation) action spectroscopy has been successfully employed to obtain the IR spectra of different amino acids^{1–19} and peptides^{12,20,21} attached to metal cations. These spectra in combination with theoretical calculations allow, for example, the determination of the more likely structures of each complex. Theoretical methods can, in addition, supply relevant information such as metal cation affinities or accurately describe the nature of the bonding. Thus, the contribution of theoretical methods to gas phase studies is indeed of great importance.

Polyglycines can be considered as the backbone of peptides and so the use of glycine oligomers as models is a logical choice for the initial analysis of the interaction of metal cations with peptides. As a result, the interaction of polyglycines, mostly glycylglycine (GG) and glycylglycylglycine (GGG), with metal cations has been considered in several works. Some of these works have been devoted to the experimental^{22–29} and theoretical^{23,24,26–31} study of the interaction of Li⁺, Na⁺, or K⁺ cation with polyglycines, mainly to estimate cation affinities. Fewer theoretical works have considered transition metal cations, calculations being performed for GG, GGG, and GGGG interacting with Ag⁺,^{32,33} Cu^{+2+/2-},^{33–35} Co⁺,³⁴ Ni⁺,^{34,36} or Fe²⁺.³⁷

Co²⁺ is an essential cation needed at trace level in organisms. However, an excess concentration of this metal cation is toxic, its accumulation or detoxification depending on the formation

of metal complexes with biological ligands such as peptides.^{38,39} Therefore, understanding the nature of the interaction between cobalt cations with peptides becomes relevant. To our knowledge, few studies on the interaction of Co cations with amino acids and peptides have been carried out. Our group has theoretically studied the interaction of Co⁺ and Co²⁺ with glycine (G).⁴⁰ This study showed that the ground-state structure of Co⁺–G corresponds to the metal cation interacting with the amino group and the carbonyl oxygen of neutral glycine. In contrast, the most stable structure for Co²⁺–G corresponds to the interaction with the carboxylate group of the zwitterionic form of glycine. Other theoretical studies on the interaction of Co²⁺ with cysteine,⁴¹ selenocysteine,⁴¹ and cysteine-containing peptides⁴² have been carried out by Tortajada's group. Moreover, the complexes of Co²⁺ with cysteine,⁴³ histidine,^{44,45} and peptides^{46,47} have also been studied by means of mass spectrometry experiments.

In this work, we present a detailed study of the interaction of Co⁺ and Co²⁺ metal cations with (glycyl)_nglycine ($n = 1–3$) as a first step to achieving a deeper insight into the intrinsic interaction between these metal cations and the backbone of peptides. In particular, we seek to determine and analyze the differences on the coordination properties of the ligands due to, on the one hand, the number of metal interacting sites (electron donor groups) and, on the other, the electronic configuration of the metal cations. Additionally, we provide the simulated IR spectra of some of the most stable structures obtained, which may be useful for IRMPD studies.

Although Co²⁺ is biologically more relevant, in biological systems transition metal ions can be found in multiple oxidation states, including the +1 charge state for cobalt.⁴⁸ The ground electronic states of Co⁺ and Co²⁺ are ³F(3d⁸) and ⁴F(3d⁷), respectively. Due to their open shell nature, the interaction of these cations with amino acids can lead to several low-lying electronic states which arise from different metal d occupation. Moreover, depending on the degree of metal complexation, the relative stability of different spin electronic states could vary. Thus, in addition to the triplet states derived from the interaction of the ³F(3d⁸) ground state of Co⁺, we have also considered the singlet state that arises from the ¹G (3d⁸) excited state of

* Corresponding authors, luis@klingon.uab.es and Mariona.Sodupe@uab.es.

Co^+ . The quintet state, arising from the $(\text{s}^1\text{d}^7)^5\text{F}$ state of Co^+ , has not been considered since, as stated in our previous work on $\text{Co}^+ - \text{glycine}$,⁴⁰ it shows a much larger repulsion between the metal and the ligand due to the 4s occupation of the metal. Thus, it is reasonable to expect that the increase in the number of basic centers coordinated to the metal cation will result in a larger destabilization of the quintet state.

Methods

In order to explore the conformational space of these kinds of systems, a previous conformational search based on $\text{Li}^+ - (\text{glycyl})_n\text{glycine}$ ($n = 1-3$) complexes has been carried out to model the electrostatic interaction of the metal cation with the polyglycines. This primary study was conducted using the Monte Carlo Multiple Minimum (MCMM) procedure,⁴⁹ with the AMBER* force field,^{50,51} as implemented in the Macromodel 7.0 package.⁵² In these calculations we have considered both the neutral form of the peptides and different zwitterionic forms (with NH_3^+ amino moiety or COH^+ amide groups). Among all the possible structures obtained, only those lying within a range of 10 kJ mol^{-1} have been used to setup the $\text{Co}^+ - (\text{glycyl})_n\text{glycine}$ starting geometries to be optimized at the DFT level. Moreover, some structures not obtained in this initial conformational search but chemically important and derived from experience with other transition metal cation systems and chemical intuition have also been computed. For Co^{2+} , the structures obtained for Co^+ have been used as starting points.

Final molecular geometries and harmonic vibrational frequencies of the considered structures have been obtained using the nonlocal hybrid three-parameter B3LYP density functional approach,⁵³⁻⁵⁵ as implemented in the Gaussian 03 program package. Previous theoretical calculations have shown that the B3LYP approach is a cost-effective method for studying transition metal-ligand systems.⁵⁶⁻⁵⁹ However, recent studies carried out in our group^{35,60-62} have demonstrated that for systems in which the spin delocalization is important, functionals with a larger percentage of exact exchange, such as BHLYP,⁶³ may provide better results compared to the highly correlated CCSD(T) method. Thus, for the most stable structures of Co^{2+} systems, in addition to B3LYP, we have also carried out BHLYP calculations.

In contrast, it has been shown⁴⁰ that the singlet-triplet separation for Co^+ -containing systems is somewhat overestimated at the B3LYP level. This overestimation is already observed in free Co^+ and deviation carries over the molecular system. Therefore, we have corrected the relative energies considering the experimental values for free Co^+ (see ref 40). The value of this correction is $-8.5 \text{ kcal mol}^{-1}$, which is the difference between the experimental singlet-triplet separation and that calculated at the B3LYP level.

Geometry optimizations and frequency calculations have been performed using the following basis set. The Co basis is based on the (14s9p5d) primitive set of Wachters⁶⁴ supplemented with one s, two p, one d diffuse functions⁶⁵ and two f polarization functions,⁶⁶ the final contracted basis set being [10s7p4d2f]. For C, N, O, and H we have used the 6-31++G(d,p) basis set. Thermodynamic corrections have been obtained assuming an ideal gas, unscaled harmonic vibrational frequencies, and the rigid rotor approximation by standard statistical methods.⁶⁷ Net atomic charges and spin densities have been obtained using the natural population analysis of Weinhold et al.^{68,69} Open shell calculations have been performed using an unrestricted formalism. All calculations have been performed with the Gaussian 03 package.⁷⁰

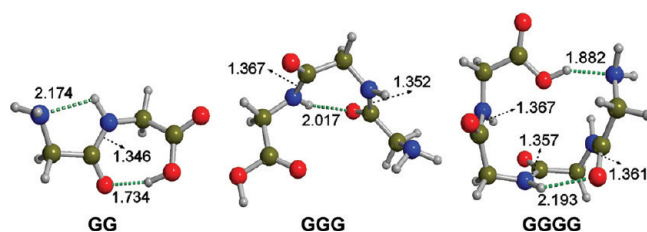


Figure 1. B3LYP optimized geometries of the most stable conformers of GG, GGG, and GGGG systems. Distances are in angstroms.

Results and Discussion

The glycylglycine, glycylglycylglycine, and glycylglycylglycylglycine peptides will be designated hereafter as GG, GGG, and GGGG, respectively. In addition, the nitrogen atom of the terminal amino group will be referred to as N_t , the oxygens and nitrogens of the peptide bonds as O_{pn} and N_{pn} , respectively, where n is the number of peptide bonds starting from the NH_2 terminus, the terminal oxygen of the carbonyl group as O_C , and the oxygen of the hydroxyl group as O_H .

Figure 1 shows the global B3LYP minima of the neutral forms of the GG, GGG, and GGGG systems, which have been located after considering the most stable and significant structures arising from previous Monte Carlo and DFT calculations. The GG conformer has been described recently as the most stable form.⁷¹ For this system as well as for the GGG and GGGG cases, other conformations were found to lie very close in energy (within a range of 1 kcal mol^{-1}). However, since the energy difference between them is very small, Co^{+2+} binding energies will not be substantially influenced whether we consider one structure or another.

The interaction of GG, GGG, and GGGG with the Co^+ and Co^{2+} leads to a large number of conformers for each system. In order to locate the preferred coordination, we have followed the strategy described in the methods section. For the sake of brevity we only show the three most stable structures of each spin and charge state. The other considered structures can be found in Figures S1–S10 of the Supporting Information.

$\text{Co}^+ - \text{GG}, -\text{GGG}, -\text{GGGG}$. For all systems, we considered the electronic states arising from both the $(\text{d}^8)^3\text{F}$ and $(\text{d}^8)^1\text{G}$ states of Co^+ . These atomic states interact with the ${}^1\text{A}$ state of $(\text{glycyl})_n\text{glycine}$ leading to a triplet ${}^3\text{A}$ and a singlet ${}^1\text{A}$ electronic state, respectively, of the $\text{Co}^+ - (\text{glycyl})_n\text{glycine}$ complexes. Tables 1 and 2 display the computed relative energies as well as the natural population analysis of the metal cation for all the obtained structures in the singlet and triplet states, respectively. Figures 2 and 3 only show the three low-lying conformers of each system ($\text{Co}^+ - \text{GG}$, $\text{Co}^+ - \text{GGG}$, or $\text{Co}^+ - \text{GGGG}$) and spin state.

Tables 1 and 2 show that triplet states of $\text{Co}^+ - (\text{glycyl})_n\text{glycine}$ complexes are more stable than the singlet ones as it happens for free Co^+ and $\text{Co}^+ - \text{G}$. For both spin states the most stable structure of the GG complexes (CoGG1_T and CoGG1_S) corresponds to the metal cation interacting with the amino nitrogen atom, the terminal carbonyl oxygen, and the amide carbonyl group ($\text{N}_t\text{O}_{p1}\text{O}_C$ coordination) of neutral GG. This structure is somewhat different to that found for other singly charged transition metal cations. For example, in the case of $\text{Cu}^+ - \text{GG}$ the cation is only coordinated to the terminal groups in a linear-like dicoordination,³⁴ due to the sd hybridization of the $d\sigma$ valence orbitals of Cu^+ .⁷² This hybridization reduces the repulsion along the metal-ligand axis and makes the coordination of a third ligand unfavorable. $\text{Ni}^+ - \text{GG}$ adopts a tricoordinated T-shape geometry but the interaction with the peptide

TABLE 1: Relative Energies Including Zero Point Corrections (ΔG_{298}° in parentheses) of the Triplet State of Co⁺–(Glycyl)_nglycine (kcal mol⁻¹) and Population Analysis at the B3LYP Level

structure	coordination	E_{rel}	$q(\text{Co})$	spin (Co)
CoGG1_T	N _t , O _{p1} , O _C	0.0 (0.0)	0.90	1.96
CoGG2_T	N _t , N _{p1} , O _C	2.0 (1.6)	0.77	1.94
CoGG3_T	N _t , O _{p1}	3.3 (1.4)	0.86	1.94
CoGG4_T	O _{p1} , O _C	5.0 (4.0)	0.90	1.95
CoGG5_T	N _t , O _{p1}	5.1 (3.7)	0.87	1.94
CoGG6_T	N _t , O _{p1}	7.2 (5.8)	0.86	1.94
CoGG7_T	N _t , N _{p1} , O _C	8.3 (7.9)	0.79	1.93
CoGG8_T	O _C , O ⁻	16.2 (14.9)	0.87	1.96
CoGG9_T	O _C , O ⁻	20.4 (18.8)	0.84	1.94
CoGG10_T	O _C , O ⁻	25.3 (24.4)	0.85	1.95
CoGGG1_T	O _{p1} , O _{p2} , O _C	0.0 (0.0)	0.95	1.98
CoGGG2_T	N _t , O _{p1} , O _{p2} , O _C	1.2 (2.0)	0.85	1.94
CoGGG3_T	N _t , O _{p1} , O _C	1.8 (1.6)	0.84	1.96
CoGGG4_T	N _t , O _{p1} , O _C	4.1 (4.0)	0.80	1.93
CoGGG5_T	N _t , O _{p1} , O _{p2}	4.5 (4.4)	0.92	1.97
CoGGG6_T	O _{p1} , N _{p2} , O _C	4.9 (4.6)	0.82	1.94
CoGGG7_T	N _t , N _{p1} , O _{p2}	5.5 (4.7)	0.75	1.94
CoGGG8_T	O _{p1} , O _{p2}	8.7 (7.6)	0.87	1.94
CoGGG9_T	N _t , N _{p1} , O _{p2} , O _C	9.3 (9.8)	0.88	1.95
CoGGG10_T	O _{p1} , O _{p2} , O _C	14.9 (15.3)	1.03	1.99
CoGGGG1_T	O _{p1} , O _{p2} , O _{p3}	0.0 (0.0)	0.97	1.99
CoGGGG2_T	O _{p1} , O _{p2} , O _{p3} , O _C	0.6 (2.2)	1.07	2.03
CoGGGG3_T	N _t , O _{p1} , O _{p3} , O _C	2.0 (2.9)	0.85	1.92
CoGGGG4_T	N _t , O _{p1} , O _{p3}	2.8 (2.7)	0.80	1.94
CoGGGG5_T	N _t , O _{p1} , O _{p2} , O _{p3}	3.2 (3.8)	0.80	1.94
CoGGGG6_T	N _t , O _{p2} , O _{p3} , O _C	12.0 (14.2)	0.85	1.91

TABLE 2: Relative Energies Including Zero Point Corrections (ΔG_{298}° in parentheses) of the Singlet State of Co⁺–(glycyl)_nglycine (kcal mol⁻¹) Calculated with Respect to the Triplet Global Minimum and Population Analysis at the B3LYP Level

structure	coordination	E_{rel}	$q(\text{Co})$
CoGG1_S	N _t , O _{p1} , O _C	17.9 (19.7)	0.86
CoGG2_S	N _t , N _{p1} , O _C	18.6 (19.6)	0.61
CoGG3_S	N _t , O _{p1}	27.5 (27.1)	0.66
CoGG5_S	N _t , O _{p1}	29.6 (29.0)	0.66
CoGG4_S	O _{p1} , O _C	31.9 (32.0)	0.76
CoGG6_S	N _t , O _{p1}	31.0 (30.7)	0.66
CoGG8_S	O _C , O ⁻	48.3 (48.1)	0.72
CoGG9_S	O _C , O ⁻	48.9 (47.7)	0.66
CoGG10_S	O _C , O ⁻	54.8 (54.7)	0.67
CoGGG1_S	O _{p1} , O _{p2} , O _C	14.4 (16.5)	0.94
CoGGG11_S	N _t , N _{p1} , N _{p2} , O _C	18.0 (20.1)	0.50
CoGGG9_S	N _t , N _{p1} , O _{p2} , O _C	19.0 (21.9)	0.71
CoGGG4_S	N _t , O _{p1} , N _{p2} , O _C	20.2 (23.2)	0.72
CoGGG5_S	N _t , O _{p1} , O _{p2}	21.8 (23.3)	0.86
CoGGG7_S	N _t , N _{p1} , O _{p2}	22.4 (23.1)	0.61
CoGGG3_S	N _t , O _{p1} , O _C	23.0 (24.2)	0.69
CoGGG6_S	O _{p1} , N _{p2} , O _C	23.0 (24.8)	0.80
CoGGG8_S	O _{p1} , O _{p2}	34.7 (34.5)	0.72
CoGGG10_S	O _{p1} , O _{p2} , O _C	45.6 (48.9)	1.02
CoGGGG3_S	N _t , O _{p1} , O _{p3} , O _C	12.1 (14.7)	0.64
CoGGGG1_S	O _{p1} , O _{p2} , O _{p3}	13.9 (15.8)	0.95
CoGGGG4_S	N _t , O _{p1} , O _{p3}	23.9 (25.7)	0.76
CoGGGG7_S	N _t , O _{p1} , N _{p3} , O _C	16.9 (20.3)	0.58
CoGGGG2_S	O _{p1} , O _{p2} , O _C	28.4 (30.2)	0.75
CoGGGG8_S	N _t , N _{p1} , N _{p3} , O _C	26.3 (30.4)	0.52
CoGGGG5_S	N _t , O _{p2} , O _{p3}	30.3 (32.2)	0.78
CoGGGG6_S	N _t , O _{p2} , O _{p3} , O _C	30.3 (35.5)	0.86

bond takes place through the nitrogen atom (N_{p1}).³⁴ Finally, Ag⁺–GG is dicoordinated and the metal cation interacts with the amino nitrogen and the amide carbonyl oxygen (N_t O_{p1}).³³ These differences arise from the different d occupation and size of each metal cation. In contrast, in the case of the alkali metal

cations the preferred structure always corresponds to the interaction of the metal cation with both carbonyl groups (O_p and O_C atoms).^{28,29}

The second most stable structure for both spin states is also tricoordinated, but the interaction with the peptide bond is established through N_{p1}. This N_tN_{p1}O_C structure is very close in energy to the N_tO_{p1}O_C one, the energy difference being 2.0 kcal mol⁻¹ for the triplet state and 0.7 kcal mol⁻¹ for the singlet state. The third structure is dicoordinated through N_t and O_{p1}, and it becomes significantly less stable in the singlet state, around 10 kcal mol⁻¹ higher in energy than the tricoordinated N_tO_{p1}O_C structure. The other computed isomers are higher in energy and are shown in Figures S1 and S4 of the Supporting Information. In particular, the zwitterionic forms correspond to the most unstable forms computed.

The ground-state structure of Co⁺–GGG is also tricoordinated in both spin states (CoGGG1_T and CoGGG1_S) but the interaction of the metal cation occurs through the three carbonyl oxygens of the peptide, similarly to alkali metal cations.^{28,29} In this case the preferred geometry is also different from that found for other singly charged transition metal cations. For Cu⁺ the global minimum is dicoordinated with the metal cation interacting with the O_C and O_{p1} atoms.^{33,35} In contrast, Ag⁺ prefers to interact with the three available carbonyl oxygens and the amino nitrogen. A similar tetracoordinated structure has been found in Co⁺–GGG (CoGGG2_T), which, for the triplet state, lies only 1.2 kcal mol⁻¹ above CoGGG1_T.

The second and third most stable structures are different for the singlet and triplet spin states due to the different metal d occupation in both states. In the case of the singlet state these structures show slightly distorted square planar-like geometry because in this spin state the metal cation has an empty d orbital in the coordination plane. This fact allows an efficient interaction between four basic centers of the peptide and the metal cation which is accompanied by a significant electron donation from the ligand to the empty d orbital. This donation is reflected in the lower metal charge of the singlet complexes in front of the triplet ones as shown in Tables 1 and 2. In contrast, in the triplet state all the d metal orbitals are occupied and the square planar coordination is not found.

The ground-state structure of Co⁺–GGGG differs from the singlet to the triplet state. In the triplet state the metal cation interacts with the three carbonyl oxygens of the peptide bonds, the coordination environment of Co⁺ being very similar to CoGGG1_T. However, in the singlet state, the increased peptide length allows the formation of a very favorable square planar coordination with the metal cation interacting with N_t, O_{p1}, O_{p3}, and O_C.

In summary, the preferred environment for Co⁺ in the triplet state is always tricoordinated. In the singlet state, as commented above, the metal cation has an empty d orbital, and in this case the square planar coordination allows the repulsion between the lone pairs of the basic centers of the ligand and the metal cation to be reduced. Therefore, when possible, the preferred coordination for the singlet state is the square planar one. That is, for Co⁺–GG the metal cation cannot adopt this type of coordination due to the short size of the ligand, but when the peptide length is increased, the tetracoordinated square planar complexes are found to be stable (Co⁺–GGG) and for the largest one, Co⁺–GGGG, the square planar coordination becomes the most stable structure. It should also be noted that the zwitterionic forms for Co⁺–polyglycines, when found, are the most unstable forms for each system (see Tables 1 and 2 and Figures S1 and S4 of the Supporting Information).

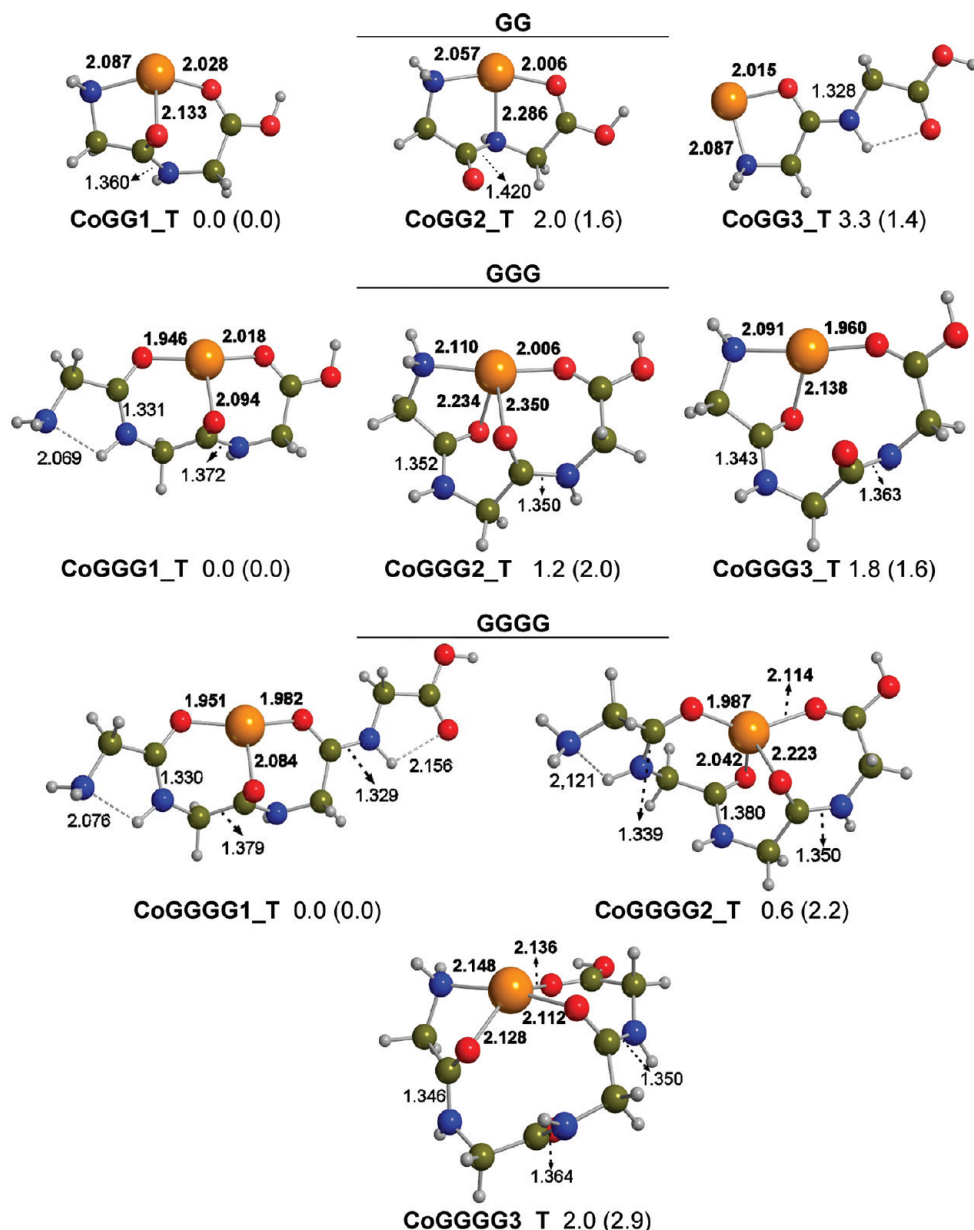


Figure 2. B3LYP optimized geometries for the low-lying conformers of the triplet state of $\text{Co}^+-(\text{glycyl})_n\text{glycine}$ and relative energies including zero point corrections (ΔG_{298}° in parentheses). Distances are in angstroms and energies in kcal mol^{-1} .

The main difference between the singlet and triplet structures corresponds to the metal–ligand distances. Due to the smaller repulsion between the singlet state of Co^+ and the peptide, metal–ligand distances are shorter than in the triplet state. The interaction with the metal cation induces changes in the backbone of the peptide. Particularly interesting are the changes produced in the peptide bond, which are somewhat more important in the singlet than in the triplet state due to the larger interaction of the basic centers of the ligand with the metal cation in the first case. Analysis of the structures shown in Figures 2 and 3 for each spin state of Co^+-GG reflects different types of activation of the peptide bond. That is, if the interaction of the metal cation takes place with the lone pair of the amide nitrogen (CoGG2_T and CoGG2_S), the neutral resonant form of the peptide bond is stabilized, inducing a lengthening of the peptide bond distance compared to that of the isolated GG. Similarly, CoGG1_T and CoGG1_S structures, in which the interaction of the metal cation occurs through the π system of the C=O bond, show a slight lengthening of the peptide bond. However, when the interaction of the metal cation with the peptide unit

takes place with the lone pairs of the carbonyl amide oxygen (CoGG3_T and CoGG3_S) the resonant zwitterionic form of the peptide bond is stabilized resulting in the shortening of the bond.

If we consider the energy difference between the triplet and singlet states of free Co^+ (${}^3\text{F}-{}^1\text{G}$ separation, 52.8 kcal mol^{-1}), $\text{Co}^+-\text{glycine}$ (26.0 kcal mol^{-1}),⁴⁰ and the $\text{Co}^+(\text{glycyl})_n\text{glycine}$ complexes considered in our study (see Table 2), it can be observed that coordination of one glycine molecule drastically reduces the energy difference (Figure S7 of the Supporting Information). As noted above, the most repulsive d orbital of the singlet state of Co^+ is empty, thus allowing a better interaction between the basic centers of the amino acid and the metal cation. The coordination of a GG molecule causes a remarkable lowering in the singlet–triplet separation because the coordination number is increased from 2 to 3. However, a further increase in the length of the peptide decreases the singlet–triplet difference to a lesser extent, the energy difference asymptotically approaching about 10 kcal mol^{-1} . Therefore, it appears that increasing the number of amino acids beyond four

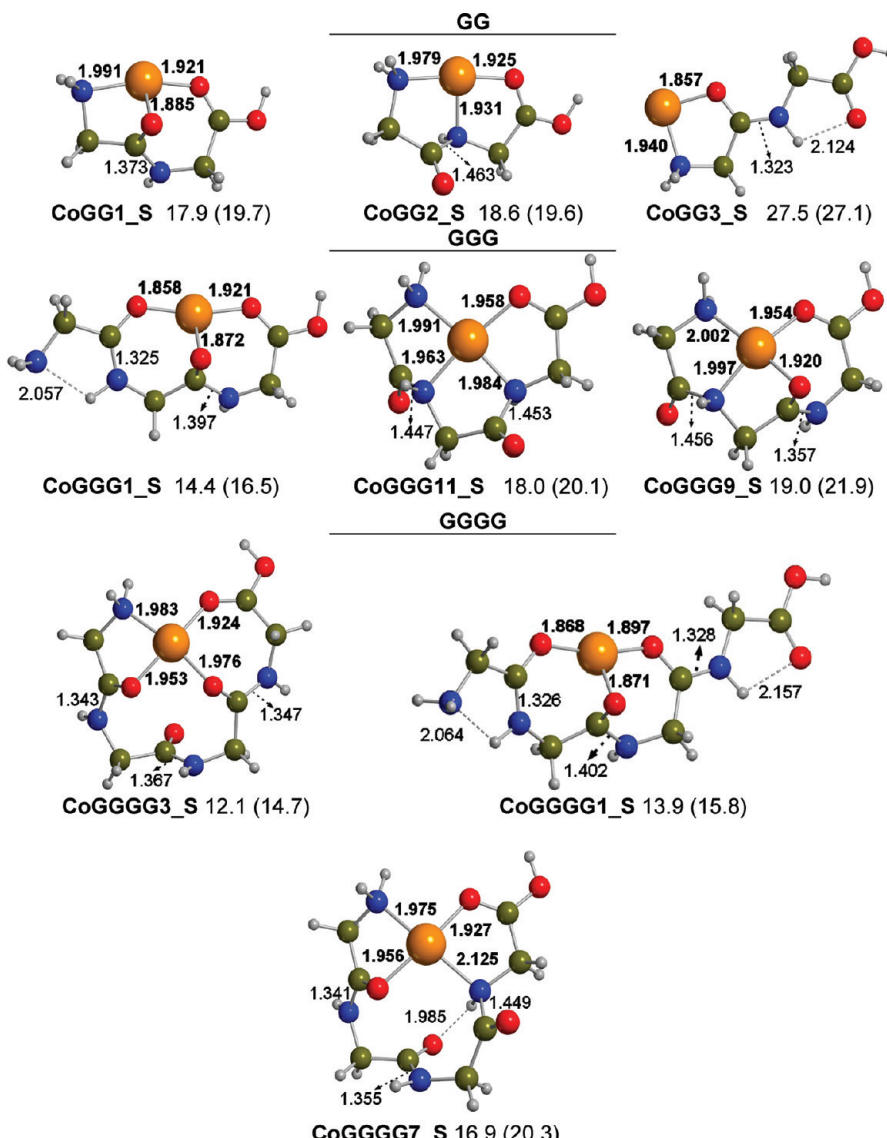


Figure 3. B3LYP optimized geometries for the low-lying conformers of the singlet state of Co⁺-(glycyl)_nglycine and relative energies including zero point corrections (ΔG_{298}° in parentheses) calculated with respect to the triplet global minimum. Distances are in angstroms and energies in kcal mol⁻¹.

will not result in an inversion of the stability between the singlet and the triplet states.

Co²⁺-GG, -GGG, -GGGG. As in the case of Co²⁺-glycine,⁴⁰ we have only considered the quartet spin state (d⁷) of Co²⁺ since doublet states are much higher in energy and coordination is not expected to reverse the doublet-quartet relative energy. In order to find the most stable structures for each coordination environment, we have followed the same procedure as for Co⁺-(glycyl)_nglycine.

Co²⁺ is a doubly charged cation, and thus the electrostatic interaction is much larger than that for Co⁺ complexes, which leads to smaller metal-ligand distances. Moreover, Co²⁺ is a d⁷ cation with three monooccupied d orbitals. In these conditions, the repulsion between the metal and the ligand is smaller than those for ³F Co⁺ (a d⁸ cation). Therefore, the interaction with more than three donor centers is expected to become more favorable. Table 3 lists the computed relative energies as well as the natural population analysis of the metal cation for all the obtained structures in the quartet state, whereas Figure 5 shows the three low-lying conformers of each system (Co²⁺-GG, Co²⁺-GGG, or Co²⁺-GGGG).

Contrary to Co⁺, for Co²⁺ the coordination number of the most stable structure increases with the number of amino acids that constitute the peptide. In fact, the most stable isomer found for each system is tricoordinated for Co²⁺-GG (CoGG1_Q), tetracoordinated for Co²⁺-GGG (CoGGG2_Q) and pentacoordinated for Co²⁺-GGGG (CoGGGG3_Q). This behavior was also observed for Cu²⁺-(glycyl)_nglycine³⁵ complexes. A further increase in the peptide length is expected to result in an octahedral coordination environment as found frequently for Co²⁺ complexes.^{73,74} In these systems, in addition to the terminal N_t and O_c atoms, the nitrogen N_p or oxygen O_p of the peptide bonds can take part of the coordination sphere. In Figure 5 it can be observed that structures in which Co²⁺ interacts with O_p are preferred to those in which Co²⁺ interacts with N_p. Indeed, the most stable conformer always involves coordination with the terminal amino group and all the available carbonyl groups, two for CoGG1_Q, three for CoGGG2_Q, and four for CoGGGG3_Q. This preference for the oxygen atom of the peptide bond was also observed for Cu²⁺-(glycyl)_nglycine³⁵ systems and is due to the fact that this interaction strengthens

TABLE 3: Relative Energies Including Zero Point Corrections (ΔG_{298}° in parentheses) of Co^{2+} –(Glycyl)_nglycine (kcal mol⁻¹) and Population Analysis at the B3LYP Level

structure	coordination	E_{rel}	$q(\text{Co})$	spin (Co)
CoGG1_Q	N _t , O _{p1} , O _C	0.0 (0.0)	1.55	2.73
CoGG11_Q	O _C , O ⁻	4.3 (1.6)	1.55	2.71
CoGG2_Q	N _t , N _{p1} , O _C	7.7 (7.1)	1.49	2.73
CoGG4_Q	O _{p1} , O _C	11.9 (11.0)	1.56	2.66
CoGG3_Q	N _t , O _{p1}	15.4 (13.9)	1.53	2.69
CoGG6_Q	N _t , O _{p1}	16.6 (15.8)	1.54	2.70
CoGG8_Q	O _C , O ⁻	26.0 (24.1)	1.55	2.71
CoGGG2_Q	N _t , O _{p1} , O _{p2} , O _C	0.0 (0.0)	1.54	2.74
CoGGG1_Q	O _{p1} , O _{p2} , O _C	10.6 (10.0)	1.56	2.70
CoGGG4_Q	N _t , O _{p1} , N _{p2} , O _C	16.0 (15.6)	1.48	2.70
CoGGG9_Q	N _t , N _{p1} , O _{p2} , O _C	22.1 (22.4)	1.47	2.69
CoGGG5_Q	N _t , O _{p1} , O _{p2}	22.3 (21.4)	1.52	2.70
CoGGG6_Q	O _{p1} , N _{p2} , O _C	24.2 (23.2)	1.50	2.71
CoGGG10_Q	O _{p1} , O _{p2} , O _C	24.5 (25.5)	1.54	2.65
CoGGG11_Q	N _t , N _{p1} , N _{p2} , O _C	27.3 (26.1)	1.43	2.70
CoGGG7_Q	N _t , N _{p1} , O _{p2}	28.1 (26.5)	1.46	2.70
CoGGG8_Q	O _{p1} , O _{p2}	30.9 (29.3)	1.54	2.65
CoGGG3_Q	N _t , O _{p1} , O _{p3} , O _{p3} , O _C	0.0 (0.0)	1.54	2.73
CoGGG2_Q	O _{p1} , O _{p2} , O _{p3} , O _C	5.9 (5.1)	1.57	2.72
CoGGG6_Q	N _t , O _{p1} , O _{p2} , O _{p3} , O _C	9.1 (9.3)	1.53	2.72
CoGGG4_Q	N _t , O _{p1} , O _{p2} , O _{p3}	11.9 (10.9)	1.52	2.73
CoGGG5_Q	N _t , O _{p1} , O _{p2} , O _{p3}	11.9 (10.9)	1.52	2.73
CoGGG7_Q	N _t , O _{p1} , O _{p2} , N _{p3} , O _C	13.2 (12.3)	1.49	2.69
CoGGG1_Q	O _{p1} , O _{p2} , O _{p3}	20.3 (18.2)	1.54	2.69

the peptide bond, as noted above for Co^+ complexes, contrary to Co^{2+} –N_p binding that shortens this bond.

As has already been noted, zwitterionic forms of Co^+ –polyglycines are the most unstable forms. However, due to the increase in the electrostatic interaction in Co^{2+} systems, for Co^{2+} –GG, the salt bridge CoGG11_Q isomer is the second most stable structure; its relative energy being only 1.6 kcal mol⁻¹ higher than that for CoGG1_Q. For Co^{2+} –GGG the zwitterionic CoGGG7_Q isomer lies 26.5 kcal mol⁻¹ above the most stable one and for Co^{2+} –GGGG no zwitterionic structures were located in the considered range of energy. Therefore, it can be concluded that as the peptide chain increases, these forms become more and more unstable. This is probably due to the fact that upon enlarging the peptide, Co^{2+} becomes more coordinated in such a way that the electrostatic interaction is reduced by a significant screening effect. Obviously, the instability shown by the Co^{2+} –zwitterion isomers may be modified by solvent effects.

It can be observed in Figure 5 that, in general, metal–ligand distances for the Co^{2+} complexes lie between those of the triplet and singlet states of Co^+ structures. This is not surprising since electrostatic interaction is greater for the Co^{2+} complexes, allowing a closer interaction between the metal and the ligand than in the triplet state of Co^+ ones. However, the presence of an empty d orbital in the singlet state of Co^+ results in shorter bonds for the triplet complexes than for the Co^{2+} ones.

Binding Energies of $\text{Co}^{+/2+}$ –GG, –GGG, –GGGG Systems. Table 4 shows the computed D_e , D_0 , ΔH_{298}° , and ΔG_{298}° values for the most stable $\text{Co}^{+/2+}$ –GG, –GGG, and –GGGG structures. In addition, the calculated interaction energies of the $\text{Co}^{+/2+}$ –G systems are also shown.

For both metal cations the binding energy increases with the number of glycine residues. Although for Co^+ the most stable structures are always tricoordinated, they differ on their metal–ligand distances. Overall, as the peptide length increases the metal–ligand distances decrease and, thus, the stabilizing electrostatic interaction is enhanced. Moreover, increasing the number of amino acid residues in the peptide chain increases

the number of Co–O_{pn} interactions (1 for CoGG1_T, 2 for CoGGG1_T, and 3 for CoGGGG1_T). As a consequence, more peptide bonds are strengthened which contributes to the increase in binding energy. It can also be observed that the value obtained for Co^+ –glycine in our previous calibration study at the B3LYP level is in good agreement with the CCSD(T) value, supporting the accuracy of the B3LYP values for the larger systems computed in this study.

In contrast, for the Co^{2+} systems, the increase in the binding energies is related to the adopted coordination geometry of the most stable isomer. As mentioned, Co^{2+} prefers to saturate its coordination environment. That is, for Co^{2+} –G, the most stable isomer is dicoordinated, for Co^{2+} –GG1_Q tricoordinated, for CoGGG2_Q tetracoordinated, and for CoGGGG3_Q pentacoordinated. Accordingly, it is not surprising to find that the binding energy follows the order of CoGGGG3_Q > CoGGG2_Q > Co²⁺–GG1_Q.

From a methodological point of view, it is worth mentioning that the computed B3LYP and CCSD(T) binding energies are in reasonable agreement for Co^+ –G and Cu^+ –G, whereas for Co^{2+} –G and Cu^{2+} –G differences are found to be significantly larger. The large difference found in the case of Cu^{2+} is attributed to the fact that some functionals (LDA, GGA, and also B3LYP) overstabilize situations in which the degree of charge and spin delocalization is important due to a bad cancellation of the self-interaction part by the exchange functional.⁷⁶ Since the admixture of exact exchange, which rigorously corrects the self-interaction, reduces the error and results with BHLYP are found to be in better agreement with the CCSD(T), we have also performed calculations using the Becke's Half and Half exchange functional for the Co^{2+} complexes. For these systems delocalization is somewhat more important than for Co^+ systems, as shown by the spin densities of Tables 1, 2, and 3. The computed BHLYP binding energies for Co^{2+} complexes are smaller than the B3LYP ones, the BHLYP value computed for Co^{2+} –G being in very good agreement with the CCSD(T) one. For Co^{2+} , the observed CCSD(T)–B3LYP variation (15 kcal mol⁻¹ for Co^{2+} –G) is, however, significantly smaller than that observed for Cu^{2+} (28 kcal mol⁻¹ for Cu^{2+} –G),⁷⁵ because in Co^{2+} systems the delocalization is less pronounced (the value of the spin density for the metal is 2.73) and therefore, the overestimation of the B3LYP value is smaller. Moreover, the difference between BHLYP and B3LYP decreases according to the length of the peptide, being only 7 kcal mol⁻¹ for the largest system. Thus, as described for Cu^{2+} , in situations in which the coordination environment of the metal cation is saturated, differences between B3LYP and BHLYP are smaller and the two functionals behave similarly.

Infrared Spectra. Figure 5 shows the IR spectra of the most stable structures of the triplet state of Co^+ –(glycyl)_nglycine and Co^{2+} –(glycyl)_nglycine complexes. The vibrational frequencies have been scaled by a 0.96 factor.⁷⁷ The most important features observed in these spectra are the following:

(i) The coordination of the terminal carbonylic oxygen (O_t) to Co^+ induces a red shift of 93 cm⁻¹ for Co^+ –GG and 86 cm⁻¹ for Co^+ –GGG, with respect to free glycine (Figure S10 of the Supporting Information), leading to an intense $\nu(\text{CO})$ stretching band. This band is not shifted in the case of Co^+ –GGGG, appearing at the same frequency of glycine (1748 cm⁻¹), because the O_t atom is not coordinated to the metal cation. For Co^{2+} complexes O_t is always coordinated to the metal cation and a red shift is observed in all cases (156 cm⁻¹ for $n = 1$, 120 cm⁻¹ for $n = 2$, and 97 cm⁻¹ for $n = 3$). It can be observed that the shift decreases significantly with the number

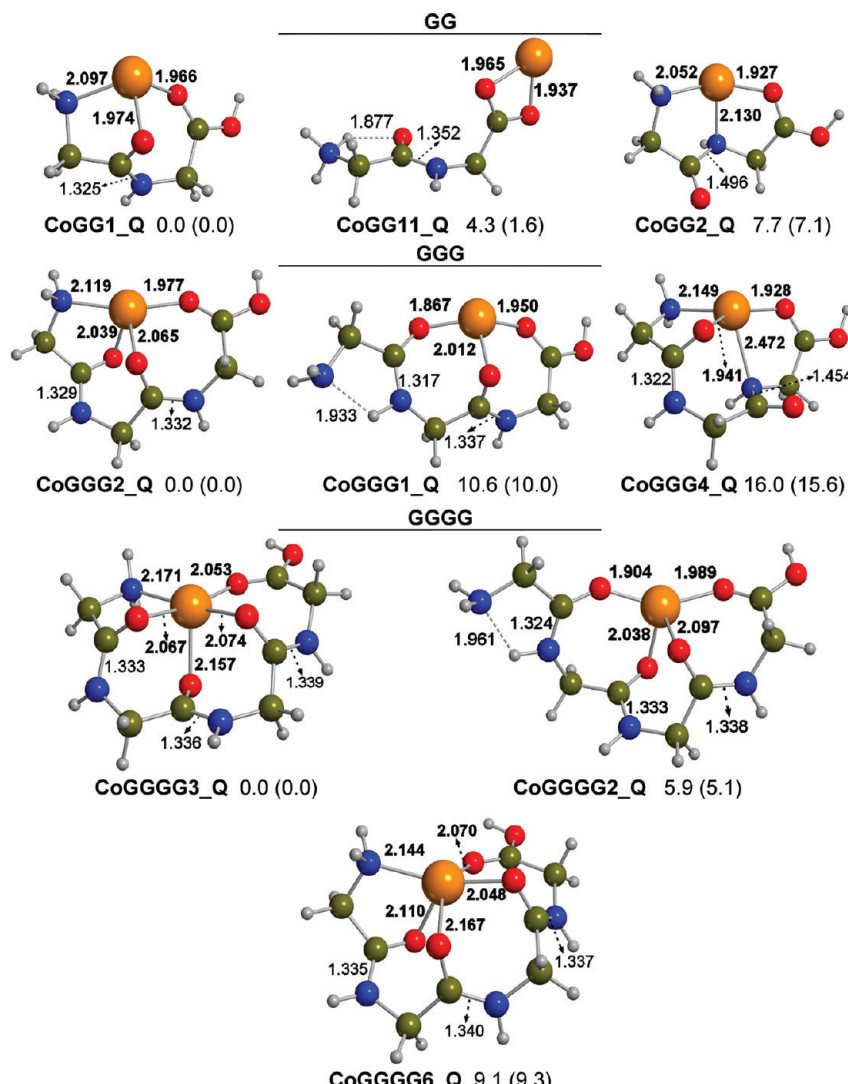


Figure 4. B3LYP optimized geometries for the low-lying conformers of Co²⁺(glycyl)_nglycine and relative energies including zero point corrections (ΔG_{298}° in parentheses) in kcal mol⁻¹.

of glycine residues because the interaction of O_t with the metal cation decreases when the peptide is enlarged. On the other hand, the intensity of the band is double in the case of Co²⁺ systems pointing out the importance of the electrostatic effects.

(ii) As regards both Co⁺ and Co²⁺ complexes, a band between 1500 and 1600 cm⁻¹ corresponding to the stretchings of the peptide bond carbonyls ($\nu(\text{CO}_{pn})$) can be observed. The intensity of this band increases with the number of residues, as the metal–O_p bond length decreases.

(iii) In the same region, but at somewhat lower frequencies, between 1470 and 1530 cm⁻¹, an intense band corresponding to the in-plane CNH bendings of the peptide bond ($\delta(\text{CN}_{pn}\text{H})$) can be observed, both for Co⁺ and for Co²⁺ complexes. If this band is not observed, for example in Co²⁺–GGG, the peaks associated to these vibrational modes are masked by the broad band of the $\nu(\text{CO}_{pn})$.

(iv) The peak corresponding to the OH stretching ($\nu(\text{OH})$) is always of moderate intensity and red-shifted with respect to free glycine (3604 cm⁻¹). The shifts in Co⁺ complexes are smaller (between 11 and 38 cm⁻¹) than in Co²⁺ (between 53 and 91 cm⁻¹) due to the large electrostatic effects in the latter systems.

(v) The region between 3300 and 3500 cm⁻¹ show bands corresponding to the symmetric and asymmetric stretchings of

the terminal NH₂ group ($\nu(\text{NH}_2)\text{a/s}$) and the NH of the peptide bond $\nu(\text{N}_{pn}\text{H})$. It can be observed that while the intensity of the $\nu(\text{NH}_2)\text{a/s}$ bands remains more or less constant, the intensity of the $\nu(\text{N}_{pn}\text{H})$ ones increases with the number of residues, so that in the spectra of the larger peptides the NH₂ stretchings are masked by the peaks of the N_{pn}H ones.

In order to facilitate the interpretation of the experimental spectra of the related system, the calculated spectra of the conformers that would likely be populated at room temperature in IRMPD experiments are included in the Supporting Information. In these spectra several features, useful to distinguish between different conformers, can be emphasized.

Co⁺–GG. The most stable structure, CoGG1_T, corresponds to the metal cation interacting with both CO groups, and consequently, the associated $\nu(\text{CO})$ and $\nu(\text{CO}_p)$ bands are considerably red-shifted compared to free glycine. In CoGG2_T, the metal cation interacts through the terminal carbonylic oxygen and the red shift of the $\nu(\text{CO})$ (1646 cm⁻¹) is similar to that found for CoGG2_T. However, the peak corresponding to $\nu(\text{CO}_p)$ (1751 cm⁻¹) is not shifted with respect to free glycine. Finally, in CoGG3_T, metal cation interaction is through the peptide carbonyl oxygen resulting in an unshifted $\nu(\text{CO})$ band (1748 cm⁻¹) and a considerably red-shifted peak for $\nu(\text{CO}_p)$

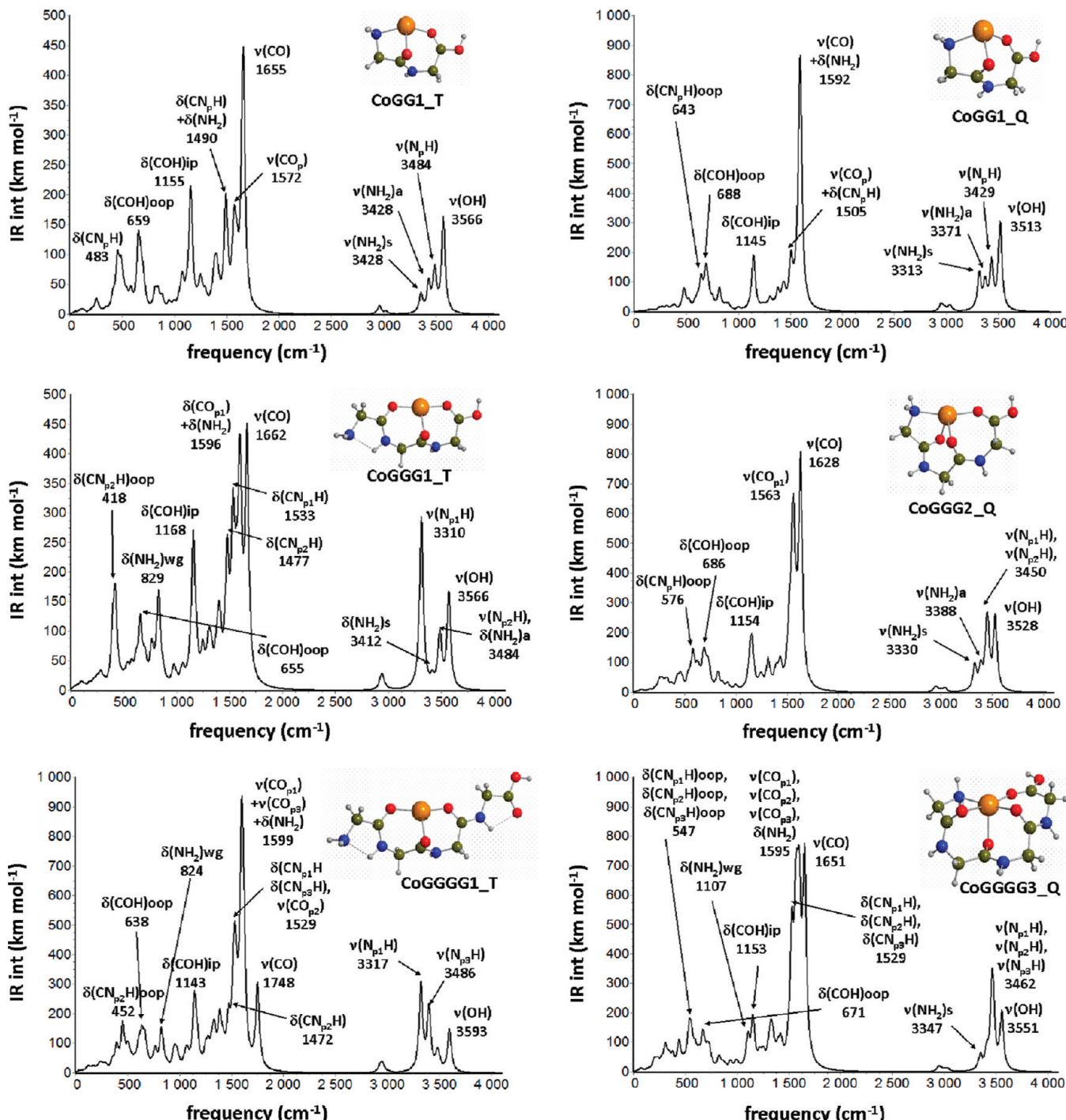


Figure 5. Computed infrared spectra for the most stable structures of the triplet state of Co^+ -(glycyl)_n-glycine and Co^{2+} -(glycyl)_n-glycine.

(1576 cm⁻¹), which can be used as a diagnostic of the presence of this conformation.

Co⁺-GGG. In this case, the spectra for the most stable conformers are very similar. The fact that the NH₂ group is not attached to Co in CoGGG1_T leads to a band associated to the wagging motion of this group ($\delta(\text{NH}_2)\text{wg} = 829$ cm⁻¹). Note that this peak is also seen in the Gly spectrum (785 cm⁻¹). In contrast, both CoGGG2_T and CoGGG3_T exhibit a direct Co–NH₂ interaction so that such a motion is not observed in their spectra. Accordingly, the presence or not of $\delta(\text{NH}_2)\text{wg}$ could be useful for the identification of the isomer formed in gas phase. On the other hand, the H-bond between N_{p1}H and the proton of N_{p1}H occurring in CoGGG1_T leads to a bathochromic shift of the band associated to $\nu(\text{N}_p\text{H})$ compared to

CoGGG2_T and CoGGG3_T (3310 vs 3485 and 3486 cm⁻¹, respectively), which in addition is more intense in the former case. The presence of this $\nu(\text{N}_p\text{H})$ intense band indicates that the NH₂ group is not interacting with Co.

Co⁺-GGGG. As in the previous case, the IR spectra in the fingerprint region are quite similar for all the conformations and could be hard to differentiate between them using IRMPD. Distinction between CoGGGG1_T and the other conformations is possible through the shift undergone by CO stretching. In the former isomer the terminal CO group is free, the $\nu(\text{CO})$ band being at 1748 cm⁻¹, as in free glycine, whereas in the others isomer CO is attached to Co, so that the $\nu(\text{CO})$ value is bathochromic shifted. On the other hand, CoGGGG1_T and CoGGGG2_T do not have the terminal NH₂ interacting with

TABLE 4: Binding Energies (D_e , D_0 , ΔH_{298}° , ΔG_{298}°) (kcal mol⁻¹) of the Co⁺²⁺-(Glycyl)_nglycine Systems (BSSE Corrected Values are in parentheses)

			G ^a	GG	GGG	GGGG
Co ⁺	D_e	B3LYP	74.2	87.2 (85.0)	98.5 (96.7)	106.0 (104.1)
		BHLYP	68.8			
		CCSD(T)	72.4			
Co ²⁺	D_e	D_0^b		85.7	97.7	106.0
		$\Delta H_{298}^\circ b$		86.5	98.3	106.2
		$\Delta G_{298}^\circ b$		76.8	87.9	98.6
Co ²⁺	D_e	B3LYP	203.3	243.5 (241.5)	287.2 (284.5)	316.8 (313.7)
		BHLYP	188.7	231.6	277.1	309.7
		CCSD(T)	190.5			
Co ²⁺	D_0^b		241.1	284.5	314.4	
		$\Delta H_{298}^\circ b$	242.3	285.9	315.6	
		$\Delta G_{298}^\circ b$	231.6	273.2	304.0	

^a Reference 40.

Co but establishing a H-bond with the proton of N_{p1}H, so that bands associated to $\delta(\text{NH}_2)\text{wg}$ (824 and 821 cm⁻¹, respectively) are present in both spectra. This is not the case in CoGGGG3_T because NH₂ is attached to Co, so that these two bands may help differentiate the formation of the first two isomers with respect to the third one.

Co²⁺–GG. According to our calculations, only two structures are likely to be populated at room temperature for this system. The most stable structure corresponds to the neutral form of GG attached to the metal cation (CoGG1_Q) and the other to the zwitterionic one (CoGG11_Q). The presence of the zwitterionic structure can be easily distinguished by the $\delta(\text{NH}_3)$ band at 1422 cm⁻¹ and the absence of the $\delta(\text{COH})_{ip}$ band in the 1150 cm⁻¹ region, typical of the neutral conformation. Additionally, in CoGG1_Q the peptide CO_p group is attached to Co whereas in CoGG11_Q it is free, so that in the former the $\nu(\text{CO}_p)$ band is found at 1595 cm⁻¹ whereas in the latter at 1698 cm⁻¹.

As aforementioned, very few IRMPD studies, mainly with alkali metal cations, have been carried out on metal cationized peptides.^{12,20,21} Among these, the work of Prell et al.²¹ addressing the interaction of alkali metal cations with ArgGly and GlyArg should be mentioned. In that study, experimental IR spectra recorded in the range of 500–2000 cm⁻¹ and theoretical calculations show that for all cases except Li⁺–ArgGly and Na⁺–ArgGly, the structure that mainly contributes to the spectrum is the zwitterionic structure of the peptide. Thereby, in these cases the recorded IR spectra are remarkably different from those calculated in our case for the most stable conformers of Co⁺–GG. In the case of Na⁺–ArgGly, both the neutral and zwitterionic structures contribute to the experimental spectrum, and theoretical calculations confirm that both structures differ by less than 1 kcal mol⁻¹ in energy. Finally, the spectrum of Li⁺–ArgGly is mainly due to the neutral conformer of the peptide. The coordination of the metal cation in this structure is very similar to that found in our case for CoGG1_T and corresponds to the interaction of the metal with the carboxylic acid carbonyl oxygen, the amide carbonyl group, and the side chain NH group of Arg. The experimental spectrum of Li⁺–ArgGly in the recorded range is similar to that found for the ground-state structure of Co⁺–GG, showing the typical bands of the nonzwitterionic structures, that is, a band at ~1150 cm⁻¹ corresponding to the in-plane COH bending and a band at 1740 cm⁻¹ corresponding to the terminal CO stretching. This band is somewhat less red-shifted (about 40 cm⁻¹) than those observed in CoGG1_T and CoGG2_T, probably due to the larger screening

effect of the NH group or to the larger charge transfer of the transition metal cations compared to the alkali ones.

However, it should be noted that, to date, these kinds of transition metal systems have not been experimentally addressed by means of the IRMPD technique so that no experimental values are available. In that respect, new experimental measurements such as those carried out by Oomens group would be welcome in order to confirm the most stable structures predicted by this work.

Conclusions

This paper analyses the interaction of Co⁺ (d⁸, ¹G, and ³F) and Co²⁺ (d⁷, ⁴F) cations with (glycyl)_nglycine (*n* = 1–3) oligomers. The structure, relative energies, and binding energies of the complexes formed have been theoretically determined by means of density functional methods. Results indicate that for all Co⁺ complexes the ground spin state is the triplet one and the most stable structure shows tricoordinated geometry. In particular, for Co⁺–GG, coordination takes place through the amino, the amide carbonyl, and the terminal carbonyl groups (N_t, O_{p1}, O_C). For Co⁺–GGG and Co⁺–GGGG, however, tricoordination takes place through three oxygen atoms, (O_{p1}, O_{p2}, O_C) and (O_{p1}, O_{p2}, O_{p3}), respectively. In contrast, for Co²⁺ systems the lowest energy structure is tricoordinated (N_t, O_{p1}, O_C) for Co²⁺–GG, tetracoordinated (N_t, O_{p1}, O_{p2}, O_C) for Co²⁺–GGG, and pentacoordinated (N_t, O_{p1}, O_{p2}, O_{p3}, O_C) for Co²⁺–GGGG. For both cobalt cations, interaction energies increase with the peptide length. Longer (glycyl)_nglycyl peptides (*n* > 3) will probably tend to have similar binding energies, as a consequence of a saturated metal coordination environment.

The infrared spectra of the low-lying structures of Co⁺–(glycyl)_nglycine and Co²⁺–(glycyl)_nglycine have been simulated. In general, it should be noted that the coordination of the carbonyl groups to the metal cation (Co⁺ or Co²⁺) induces an important red shift of the corresponding CO stretching frequency. Thereby, the presence of an unshifted peak in the region of 1750 cm⁻¹ can be used as a signature of the population of conformers with one of the carbonyl groups not coordinated to the metal cation. This is the case of Co⁺–GG where the spectra of the excited conformers, CoGG2_T and CoGG3_T, show peaks at 1751 and 1748 cm⁻¹, respectively. For Co⁺–GGG and Co⁺–GGGG, the computed spectra of the different low-energy conformers are similar in the fingerprint region. For the former case, the most stable structure can be distinguished by the presence of the band associated to the wagging motion of the NH₂ group ($\delta(\text{NH}_2)\text{wg}$ = 829 cm⁻¹), due to the fact that the NH₂ group is not attached to Co in CoGGG1_T. For Co⁺–GGGG, the low-energy structure is characterized by the unshifted $\nu(\text{CO})$ band at 1748 cm⁻¹ not present in the rest of the conformers. Finally, for Co²⁺ complexes, only Co²⁺–GG shows more than one structure that is likely to be populated at room temperature. In this case the excited conformer (CoGG11_Q) corresponds to the zwitterionic form of the ligand and can be easily identified by the presence of the $\delta(\text{NH}_3)$ band at 1422 cm⁻¹ and the absence of the $\delta(\text{COH})_{ip}$ band in the 1150 cm⁻¹ region.

Acknowledgment. Financial support from MCYT and DURSI, through the CTQ2008-06381/BQU and SGR2005-00244 projects, and the use of the Catalonia Supercomputer Centre (CESCA) are gratefully acknowledged.

Supporting Information Available: Optimized geometries for the all minima of Co⁺²⁺–(glycyl)_nglycine, computed infrared spectra of the most stable conformers of each system, and computed infrared spectrum of glycine. This material is available free of charge via the Internet at <http://pubs.acs.org>.

References and Notes

- (1) Dunbar, R. C.; Steill, J. D.; Polfer, N. C.; Oomens, J. *J. Phys. Chem. A* **2009**, *113*, 845.
- (2) Bush, M. F.; Oomens, J.; Williams, E. R. *J. Phys. Chem. A* **2009**, *113*, 431.
- (3) Drayss, M. K.; Blunk, D.; Oomens, J.; Schaefer, M. *J. Phys. Chem. A* **2008**, *112*, 11972.
- (4) O'Brien, J. T.; Prell, J. S.; Steill, J. D.; Oomens, J.; Williams, E. R. *J. Phys. Chem. A* **2008**, *112*, 10823.
- (5) Bush, M. F.; Oomens, J.; Saykally, R. J.; Williams, E. R. *J. Phys. Chem. A* **2008**, *112*, 8578.
- (6) Dunbar, R. C.; Polfer, N. C.; Oomens, J. *J. Am. Chem. Soc.* **2007**, *129*, 14562.
- (7) Forbes, M. W.; Bush, M. F.; Polfer, N. C.; Oomens, J.; Dunbar, R. C.; Williams, E. R.; Jockusch, R. A. *J. Phys. Chem. A* **2007**, *111*, 11759.
- (8) Bush, M. F.; Forbes, M. W.; Jockusch, R. A.; Oomens, J.; Polfer, N. C.; Saykally, R. J.; Williams, E. R. *J. Phys. Chem. A* **2007**, *111*, 7753.
- (9) Polfer, N. C.; Oomens, J.; Dunbar, R. C. *Phys. Chem. Chem. Phys.* **2006**, *8*, 2744.
- (10) Kapota, C.; Lemaire, J.; Maitre, P.; Ohanessian, G. *J. Am. Chem. Soc.* **2004**, *126*, 1836.
- (11) Polfer, N. C.; Oomens, J.; Moore, D. T.; Von Helden, G.; Meijer, G.; Dunbar, R. C. *J. Am. Chem. Soc.* **2006**, *128*, 517.
- (12) Polfer, N. C.; Paizs, B.; Snoek, L. C.; Compagnon, I.; Suhai, S.; Meijer, G.; Von Helden, G.; Oomens, J. *J. Am. Chem. Soc.* **2005**, *127*, 8571.
- (13) Bush, M. F.; Forbes, M. W.; Jockusch, R. A.; Oomens, J.; Polfer, N. C.; Saykally, R. J.; Williams, E. R. *J. Phys. Chem. A* **2007**, *111*, 7753.
- (14) Armentrout, P. B.; Rodgers, M. T.; Oomens, J.; Steill, J. D. *J. Phys. Chem. A* **2008**, *112*, 2248.
- (15) Bush, M. F.; O'Brien, J. T.; Prell, J. S.; Saykally, R. J.; Williams, E. R. *J. Am. Chem. Soc.* **2007**, *129*, 1612.
- (16) Bush, M. F.; Prell, J. S.; Saykally, R. J.; Williams, E. R. *J. Am. Chem. Soc.* **2007**, *129*, 13544.
- (17) Kamarotis, A.; Boyarkin, O. V.; Mercier, S. R.; Beck, R. D.; Bush, M. F.; Williams, E. R.; Rizzo, T. R. *J. Am. Chem. Soc.* **2006**, *128*, 905.
- (18) Rodgers, M. T.; Armentrout, P. B.; Oomens, J.; Steill, J. D. *J. Phys. Chem. A* **2008**, *112*, 2258.
- (19) Armentrout, P. B.; Rodgers, M. T.; Oomens, J.; Steill, J. D. *J. Phys. Chem. A* **2008**, *112*, 2248.
- (20) Polfer, N. C.; Oomens, J.; Dunbar, R. C. *ChemPhysChem* **2008**, *9*, 579.
- (21) Prell, J. S.; Demireva, M.; Oomens, J.; Williams, E. R. *J. Am. Chem. Soc.* **2009**, *131*, 1232.
- (22) Klassen, J. S.; Anderson, S. G.; Blades, A. T.; Kebarle, P. *J. Phys. Chem.* **1996**, *100*, 14218.
- (23) Cerda, B. A.; Hoyau, S.; Ohanessian, G.; Wesdemiotis, C. *J. Am. Chem. Soc.* **1998**, *120*, 2437.
- (24) Wyttenbach, T.; Bushnell, J. E.; Bowers, M. T. *J. Am. Chem. Soc.* **1998**, *120*, 5098.
- (25) Feng, W. Y.; Gronert, S.; Lebrilla, C. B. *J. Am. Chem. Soc.* **1999**, *121*, 1365.
- (26) Kish, M. M.; Wesdemiotis, C.; Ohanessian, G. *J. Phys. Chem. B* **2004**, *108*, 3086.
- (27) Wang, P.; Wesdemiotis, C.; Kapota, C.; Ohanessian, G. *J. Am. Soc. Mass Spectrom.* **2007**, *18*, 541.
- (28) Ye, S. J.; Armentrout, P. B. *J. Phys. Chem. A* **2008**, *112*, 3587.
- (29) Balaj, O. P.; Kapota, C.; Lemaire, J.; Ohanessian, G. *Int. J. Mass Spectrom.* **2008**, *269*, 196.
- (30) Wong, C. H. S.; Ma, N. L.; Tsang, C. W. *Chem.—Eur. J.* **2002**, *8*, 4909.
- (31) Benzakour, M.; McHarfi, M.; Cartier, A.; Daoudi, A. *J. Mol. Struct. (THEOCHEM)* **2004**, *710*, 169.
- (32) Chu, I. K.; Shoeib, T.; Guo, X.; Rodriguez, C. F.; Lau, T.-C.; Hopkinson, A. C.; Siu, M. K. W. *J. Am. Soc. Mass Spectrom.* **2001**, *12*, 163.
- (33) Shoeib, T.; Rodriguez, C. F.; Siu, K. W. M.; Hopkinson, A. C. *Phys. Chem. Chem. Phys.* **2001**, *3*, 853.
- (34) Constantino, E.; Rimola, A.; Rodriguez-Santiago, L.; Sodipe, M. *New J. Chem.* **2005**, *29*, 1585.
- (35) Rimola, A.; Constantino, E.; Rodriguez-Santiago, L.; Sodipe, M. *J. Phys. Chem. A* **2008**, *112*, 3444.
- (36) Xu, J. H.; Hu, C. W. *Acta Chim. Sin.* **2006**, *64*, 1622.
- (37) Xu, J. J. *Mol. Struct. (THEOCHEM)* **2005**, *757*, 171.
- (38) Cobbett, C. S. *Plant Physiol.* **2000**, *123*, 825.
- (39) Cobbett, C. S. *Curr. Opin. Plant Biol.* **2000**, *3*, 211.
- (40) Constantino, E.; Rodriguez-Santiago, L.; Sodipe, M.; Tortajada, J. *J. Phys. Chem. A* **2005**, *109*, 224.
- (41) Spezia, R.; Tournois, G.; Cartailler, T.; Tortajada, J.; Jeanvoine, Y. *J. Phys. Chem. A* **2006**, *110*, 9727.
- (42) Spezia, R.; Tournois, G.; Tortajada, J.; Cartailler, T.; Gaigeot, M.-P. *Phys. Chem. Chem. Phys.* **2006**, *8*, 2040.
- (43) Buchmann, W.; Spezia, R.; Tournois, G.; Cartailler, T.; Tortajada, J. *J. Mass Spectrom.* **2007**, *42*, 517.
- (44) Lavanant, H.; Hecquet, E.; Hoppilliard, Y. *Int. J. Mass Spectrom.* **1999**, *185/186/187*, 11.
- (45) Hu, P.; Loo, J. A. *J. Am. Chem. Soc.* **1995**, *117*, 11314.
- (46) Peifeng, H.; Sorensen, C.; Gross, M. L. *J. Am. Soc. Mass Spectrom.* **1995**, *6*, 1079.
- (47) Cerda, B. A.; Cornett, L.; Wesdemiotis, C. *Int. J. Mass Spectrom.* **1999**, *193*, 205.
- (48) Cowan, J. A. *Inorganic Biochemistry: An Introduction*; VCH: New York, 1993.
- (49) Saunders, M.; Houk, K. N.; Wu, Y. D.; Still, W. C.; Lipton, M. J. *J. Am. Chem. Soc.* **1990**, *112*, 1419.
- (50) Weiner, S. J.; Kollman, P. A.; Case, D. A.; Singh, U. C.; Ghio, C.; Alagona, G.; Profeta, S., Jr.; Weiner, P. *J. Am. Chem. Soc.* **1984**, *106*, 765.
- (51) Weiner, S. J.; Kollman, P. A.; Nguyen, D. T.; Case, D. A. *J. Comput. Chem.* **1986**, *7*, 230.
- (52) Mohamadi, F.; Richards, N. G. J.; Guida, W. C.; Liskamp, R.; Lipton, M.; Caufield, C.; Chang, G.; Hendrickson, T.; Still, W. C. *J. Comput. Chem.* **1990**, *11*, 440.
- (53) Becke, A. D. *J. Chem. Phys.* **1993**, *98*, 5648.
- (54) Lee, C.; Yang, W.; Parr, R. G. *Phys. Rev. B* **1988**, *37*, 785.
- (55) Stephens, P. J.; Devlin, F. J.; Chabalowski, C. F.; Frisch, M. J. *J. Phys. Chem.* **1994**, *98*, 11623.
- (56) Bauschlicher, C. W.; Ricca, A.; Partridge, H.; Langhoff, S. R. *Recent Advances in Density Functional Theory. Part II*; World Scientific Publishing Co.: Singapore, 1997.
- (57) Blomberg, M. R. A.; Siegbahn, P. E. M.; Svensson, M. *J. Chem. Phys.* **1996**, *104*, 9546.
- (58) Holthausen, M. C.; Mohr, M.; Koch, W. *Chem. Phys. Lett.* **1995**, *240*, 245.
- (59) Luna, A.; Alcamí, M.; Mó, O.; Yáñez, M. *Chem. Phys. Lett.* **2000**, *320*, 129.
- (60) Georgieva, I.; Tredafilova, N.; Rodriguez-Santiago, L.; Sodipe, M. *J. Phys. Chem. A* **2005**, *109*, 5668.
- (61) Poater, J.; Sola, M.; Rimola, A.; Rodriguez-Santiago, L.; Sodipe, M. *J. Phys. Chem. A* **2004**, *108*, 6072.
- (62) Rimola, A.; Rodriguez-Santiago, L.; Sodipe, M. *J. Phys. Chem. B* **2006**, *110*, 24189.
- (63) Becke, A. D. *J. Chem. Phys.* **1993**, *98*, 1372.
- (64) Wachters, A. J. *J. Chem. Phys.* **1970**, *52*, 1033.
- (65) Hay, P. J. *J. Chem. Phys.* **1977**, *66*, 4377.
- (66) Raghavachari, K.; Trucks, G. W. *J. Chem. Phys.* **1989**, *91*, 1062.
- (67) McQuarrie, D. *Statistical Mechanics*; Harper and Row: New York, 1986.
- (68) Reed, A. E.; Curtiss, L. A.; Weinhold, F. *Chem. Rev.* **1988**, *88*, 899.
- (69) Weinhold, F.; Carpenter, J. E. *The Structure of Small Molecules and Ions*; Plenum: New York, 1988.
- (70) Frisch, M. J.; Trucks, G. W.; Schlegel, H. B.; Scuseria, G. E.; Robb, M. A.; Cheeseman, J. R.; Montgomery, J. A., Jr.; Kudin, K. N.; Burant, J. C.; Millam, J. M.; Iyengar, S. S.; Tomasi, J.; Barone, V.; Mennucci, B.; Cossi, M.; Scalmani, G.; Rega, N.; Petersson, G. A.; Nakatsuji, H.; Hada, M.; Ehara, M.; Toyota, K.; Fukuda, R.; Hasegawa, J.; Ishida, M.; Nakajima, T.; Honda, Y.; Kitao, O.; Nakai, H.; Klene, M.; Li, X.; Knox, J. E.; Hratchian, H. P.; Cross, J. B.; Adamo, C.; Jaramillo, J.; Gomperts, R.; Stratmann, R. E.; Yazyev, O.; Austin, A. J.; Cammi, R.; Pomelli, C.; Ochterski, J. W.; Ayala, P. Y.; Morokuma, K.; Voth, G. A.; Salvador, P.; Dannenberg, J. J.; Zákrzewski, V. G.; Dapprich, S.; Daniels, A. D.; Strain, M. C.; Farkas, O.; Malick, D. K.; Rabuck, A. D.; Raghavachari, K.; Foresman, J. B.; Ortiz, J. V.; Cui, Q.; Baboul, A. G.; Clifford, Cioslowski, J.; Stefanov, B. B.; Liu, G.; Liashenko, A.; Piskorz, P.; Komaromi, I.; Martin, R. L.; Fox, D. J.; Keith, T.; Al-Laham, M. A.; Peng, C. Y.; Nanayakkara, A.; Challacombe, M.; Gill, P. M. W.; Johnson, B.; Chen, W.; Wong, M. W.; Gonzalez, C.; Pople, J. A. *Gaussian 03, Rev. C.02 ed.*; Gaussian Inc.: Wallingford, CT, 2003.
- (71) Gil, A.; Bertran, J.; Sodipe, M. *J. Chem. Phys.* **2006**, *124*, 154306.
- (72) Bauschlicher, C. W., Jr.; Langhoff, S. R.; Partridge, H. *J. Chem. Phys.* **1991**, *94*, 2068.
- (73) Huheey, J. E.; Keiter, E. A.; Keiter, R. L. *Inorganic Chemistry: Principles of Structure and Reactivity*, 4th ed.; HarperCollins College Publishers: New York, 1993.
- (74) Wilkins, P. C.; Wilkins, R. G. *Inorganic Chemistry in Biology*; Oxford University Press: Oxford, 1997.
- (75) Bertran, J.; Rodriguez-Santiago, L.; Sodipe, M. *J. Phys. Chem. B* **1999**, *103*, 2310.
- (76) Sodipe, M.; Bertran, J.; Rodriguez-Santiago, L.; Baerends, E. J. *J. Phys. Chem. A* **1999**, *103*, 166.
- (77) Scott, A. P.; Radom, L. *J. Phys. Chem.* **1996**, *100*, 16502.